Dynamics of photoinduced melting of charge/orbital order in a layered manganite $La_{0.5}Sr_{1.5}MnO_4$

T. Ogasawara,[1,2] T. Kimura,[1,3] T. Ishikawa,[1,*] M. Kuwata-Gonokami,[1] and Y. Tokura[1,2,3]
[1]*Department of Applied Physics, University of Tokyo, Tokyo 113-8656, Japan*
[2]*Correlated Electron Research Center (CERC), Tsukuba 305-0046, Japan*
[3]*Joint Research Center for Atom Technology (JRCAT), Tsukuba 305-0046, Japan*
(Received 7 August 2000; published 1 March 2001)

Photoinduced effects on the charge- and orbital-ordered (CO/OO) states in a layered perovskite manganite $La_{0.5}Sr_{1.5}MnO_4$ have been investigated with femtosecond polarization-sensitive pump-probe spectroscopy. Disappearance of the optical birefringence as well as conspicuous change of the optical spectrum indicates the immediate destruction of the CO/OO states upon photoexcitation. A large difference in the temporal evolution of the birefringence and the reflectivity change was observed, indicating that the adiabatic, fast (<200 fs) photomelting of the CO/OO states is followed by slow (10 ps–10 ns) evolution of the lattice disorder, which is subject to the critical slowing down effect as the temperature approaches $T_{CO}=220$ K.

DOI: 10.1103/PhysRevB.63.113105 PACS number(s): 78.47.+p, 73.22.−f, 71.30.+h

Charge and orbital ordering phenomena in transition-metal oxides, such as $La_{2-x}Sr_xNiO_{4+\delta}$,[1,2] $La_{2-x-y}Nd_ySr_xCuO_4$,[3] and many perovskite manganites,[4] have attracted much attention in recent years. Among them, charge/orbital ordering or correlation coupled with the collective Jahn-Teller lattice distortion are now believed to be essential for the phenomenon of colossal magnetoresistance (CMR) in the manganites.[4,5] As far as the ground state of the CMR manganite is concerned, the charge/orbital ordering and the collective Jahn-Teller distortion are strongly tied to each other, and it seems very hard to distinguish these two. However, the dynamical properties may be different because of the different origin (i.e., electronic vs lattice) of these types of order. To discriminate their respective dynamics, femtosecond spectroscopy is a promising method, as its temporal resolution almost reaches the typical time scale of electron motion in a solid.[6]

Rich electronic and structural phases diagrams in CMR manganites also offer a good arena to pursue the possibility of photocontrol of material phases, which is of great interest.[7–10] As the typical photon energy of the exciting light is much larger than the characteristic energy scales relevant to the phase transition, photoexcitation may create a nonequilibrium state that evolves into another (meta) stable state across the thermally inaccessible potential barrier of the free energy. The phenomena of charge and orbital ordering/disordering in manganites are particularly suitable for this purpose. First, the optical anisotropy induced by the orbital ordering enables us to observe the ordered-state or disordered-state region directly by optical means. Second, since the electrons relevant to the charge and orbital ordering directly respond to the optical-energy (~ 1 eV) photons, the charge and orbital order should be perturbed effectively upon photoillumination. Furthermore, the electronic as well as magnetic properties of these materials are closely related to the charge/orbital order, so that interesting photoswitching of these properties is also anticipated.

In this Brief Report, we describe investigations of photoinduced changes of charge- and orbital-ordered (CO/OO) states in a layered-structure manganite $La_{0.5}Sr_{1.5}MnO_4$, which shows the ideally simple tetragonal (square lattice) structure at room temperature. We have observed ultrafast (<200 fs) melting of the CO/OO state upon photoexcitation as well as separated dynamics of the order parameters for the charge/orbital order and the lattice deformation (Jahn-Teller distortion), which are otherwise strongly tied to each other.

In $La_{0.5}Sr_{1.5}MnO_4$, nominal Mn^{3+} and Mn^{4+} sites are generated in a 1:1 ratio,[11] and a checkerboard type charge-ordered state appears below $T_{CO}=220$ K.[12] Upon this transition, an orbital-ordered (OO) state emerges concomitantly, where the $3x^2-r^2$ and $3y^2-r^2$ orbitals of the e_g electrons line up in the manner as shown in Fig. 1(a).[13] Although simple charge ordering would keep the tetragonal symmetry D_{4h}, the concomitant orbital ordering changes it to D_{2h}, causing optical anisotropy in the Mn-O plane. This can be discerned in Fig. 1(a) as the inequivalent orbital ordering along the a' axis (uniform) and along the b' axis (staggered). The orbital ordering accompanies a collective Jahn-Teller type distortion, which shows up clearly in Raman and infrared phonon spectra.[14,15] The CO/OO state below $T_{CO}=220$ K undergoes an antiferromagnetic spin-ordering transition at $T_N=110$ K. Both the CO/OO transition and the antiferromagnetic transition are three-dimensional (3D) in nature with long-range order,[12,13] although a strong fluctuation of the CO/OO states persists far above T_{CO}, reflecting the 2D nature.[14]

The charge/orbital ordering and the associated collective Jahn-Teller distortion can also be observed as optical anisotropy by probing the polarization change of reflected light. When the polarization of the incident light is parallel to the a (b) axis, the reflectivity of the polarization perpendicular to the incident light is[16] $R_\perp=\frac{1}{2}|r_{a'}-r_{b'}|^2$, where $r_{a'}$ and $r_{b'}$ are the complex reflectivities for polarization parallel to the a' and b' axes, respectively. In fact, it was confirmed that $R_\perp/R$ at 1.96 eV shows nearly parallel T dependence to that of the order parameter derived from diffraction measurements.[15]

A single crystal of $La_{0.5}Sr_{1.5}MnO_4$ was grown by the floating zone method, and a flat ab surface was cleaved from the crystal boule for optical measurements. Polarization microscope images of the ab plane for the ordered phase (T

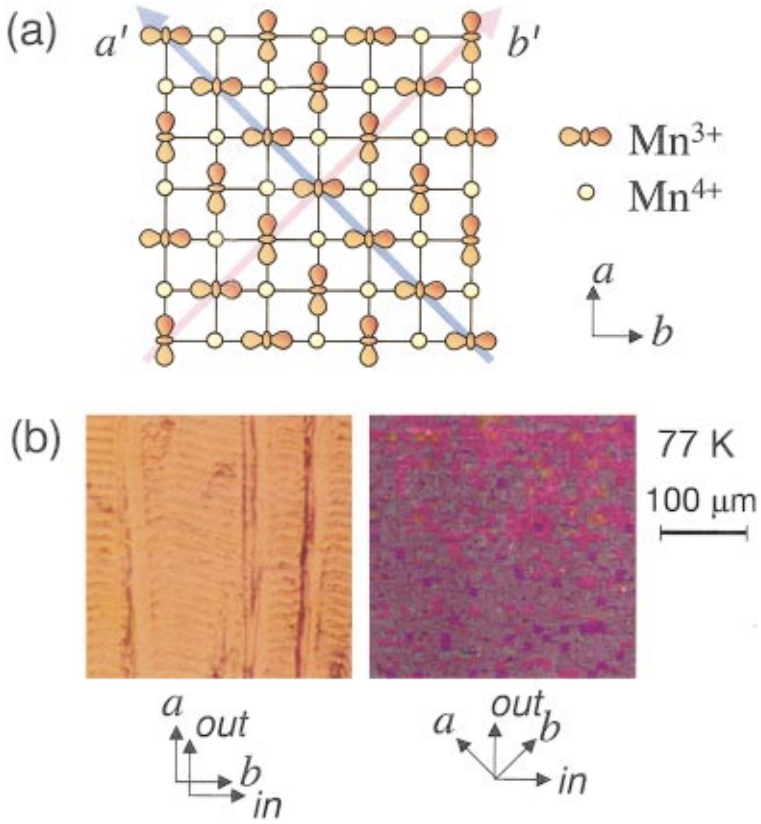

FIG. 1. Color (a) Schematic picture of charge- and orbital-ordering pattern on the ab plane of $La_{0.5}Sr_{1.5}MnO_4$. The anisotropy arises from the difference between the orbital order and the associated collective lattice distortion along the a' axis and along the b' axis. (b) Polarization microscope images in cross-Nichol configurations for the ordered phase at 77 K indicating the optical anisotropy with the optical principal axes of a' and b'. The contrast of the right-side image, which is almost invisible, is enhanced approximately $\times 10$ with respect to the left one.

$=77$ K) are shown in Fig. 1(b). The relationship between the polarization and the crystal axes is denoted in the figure. One can see a bright image in the ordered phase because of the optical anisotropy or birefringence due to CO/OO when the polarizations of incident and reflected light are parallel to the a and b axes, respectively. This bright image turns into a dark one when the temperature is raised above T_{CO} $(=220$ K), or when the light polarizations are each rotated by 45° to coincide with the optical principal axes, the a' and b' axes [the right panel of Fig. 1(b)]. The characteristic stripe pattern observed in the ordered phase is considered as a domain structure [the orbital order has two equivalent domains, that shown in Fig. 1(a) and its mirror image] which seems to be fixed by the crystal habit embedded during crystal growth. The bright area is the single domain of orbital order, while the dark lines correspond to disordered or corrugated small-domain areas such as the domain wall.

Photoinduced effects have been investigated by a polarization-sensitive time-resolved pump-probe method. An amplified mode-locked Ti:sapphire laser (800 nm in center wavelength, 150 fs in pulse duration, and 1 kHz in repetition rate) was used as a pump light source, and an optical parametric amplifier with second and fourth harmonic generators (400–2500 nm in center wavelength and 200 fs in pulse duration) as a probe light source.

Spectra of the reflectivity change $\Delta R/R$ at 10 K induced by photoexcitation (~ 150 μJ/cm^2) are shown in Fig. 2(a) for various probe delay times. Quite a large reflectivity change up to 25% is observed over the measured photon energy region (0.5–3.0 eV). The corresponding optical conductivity spectra obtained by the Kramers-Kronig transfor-

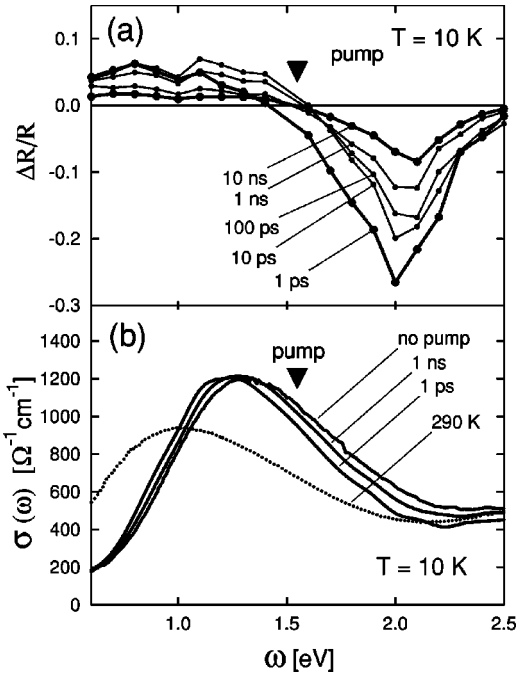

FIG. 2. (a) Spectra of reflectivity change $\Delta R/R$ upon photoexcitation at 10 K at various probe delays from 1 ps to 10 ns. The pump photon energy is 1.55 eV (indicated with closed downward triangles), and the excitation intensity is ~ 150 μJ/cm^2. (b) The corresponding optical conductivity spectra obtained from a Kramers-Kronig transformation at the delay times of 1 ps and 1 ns. The optical conductivity spectrum at 290 K (as typical of a high-temperature charge/orbital-disordered state) is also shown with a dotted line for comparison.

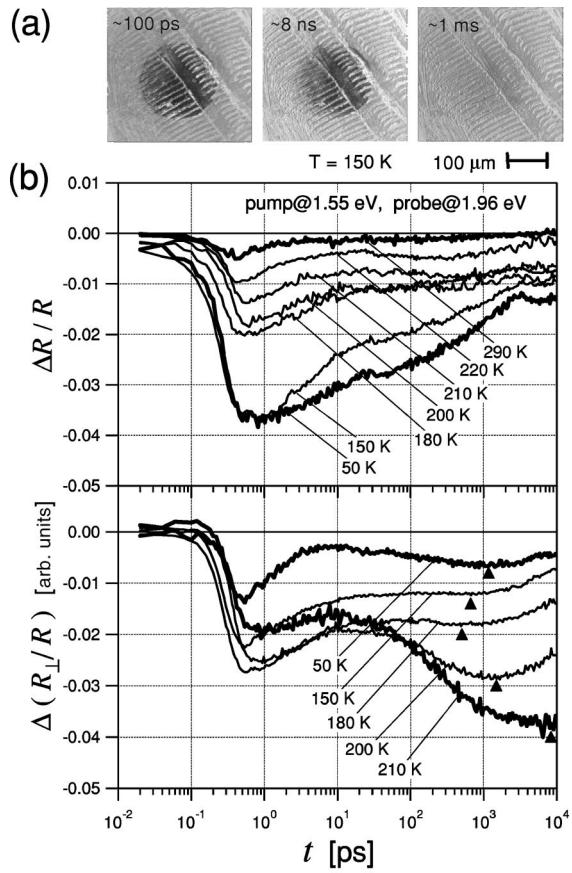

FIG. 3. (a) Time-resolved polarization microscope images $[\Delta(R_\perp/R)$ images] at 150 K. The last image corresponds to a negative probe delay that delays the probe by 1 ms after the previous pump pulse. (b) Temporal evolution of the differential reflectivity $\Delta R/R$ (upper panel) and the change of anisotropy $\Delta(R_\perp/R)$ (lower panel) at various temperatures. The pump and probe photon energies are 1.55 eV and 1.96 eV, respectively. The closed triangles denote the positions of the $|\Delta(R_\perp/R)|_{\max}$ and $t_{\max}$ plotted in Fig. 4.

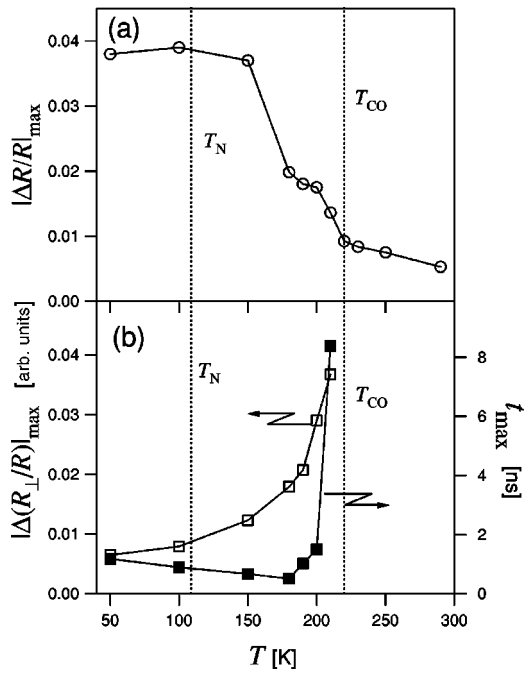

FIG. 4. Temperature dependence of the characteristic values found in Fig. 3: (a) the initial peak value $|\Delta R/R|_{\max}$, and (b) the delayed-peak value $|\Delta(R_\perp/R)|_{\max}$ and its delay time $t_{\max}$. The vertical broken lines represent T_N and T_{CO} for the antiferromagnetic spin transition and the charge/orbital-ordering transition, respectively. Solid lines are merely guides to the eyes.

mation are shown in Fig. 2(b). To perform the Kramers-Kronig transformation, the photoinduced reflectivity spectra were smoothly connected to the static reflectivity spectra at both the lower and higher energy sides. The broad peak around 1.3 eV, which corresponds to charge transfer excitation of e_g electrons from Mn^{3+} to Mn^{4+} sites,[15] shifts to lower energy with photoexcitation, signaling that the CO/OO state is modified by photoexcitation. In the thermally disordered phase at 290 K, broadening of the peak is observed in the static optical conductivity spectrum[15] as seen in Fig. 2(b), whereas narrowing is observed upon photoexcitation. This indicates that the photoexcitation effect is not due to simple heating.

As mentioned above, the orbital ordering manifests itself in the optical birefringence. Making use of this feature, the temporal evolution of orbital disordering caused by a pulsed photoexcitation can be probed by monitoring the polarization change of the probe light. Figure 3(a) shows the time-resolved images of $\Delta(R_\perp/R)$ observed at 150 K (the last image corresponds to a negative probe delay where the probe pulse is delayed by 1 ms from the previous pump pulse). The pump and probe photon energies are 1.55 eV and 1.96 eV, respectively. The stripe pattern is the same as shown in Fig. 1(b) left. The central circular region is the pump-illuminated area. Darkened images representing the decrease of $R_\perp/R$ clearly indicate that the CO/OO state is destroyed by photoexcitation in this area.

The temporal evolution of the differential reflectivity $\Delta R/R$ and the anisotropy change $\Delta(R_\perp/R)$ probed at 1.96 eV is shown in Fig. 3(b). The photoexcitation is carried out at 1.55 eV. The excitation pulse energy is $\sim 30\ \mu J/cm^2$. For the convenience of plotting on a logarithmic time scale, the temporal origin is tentatively set at 200 fs prior to the initial edge of the signal, which actually almost coincides with the probe pulse width of 200 fs. The signal intensity is approximately proportional to the excitation intensity. Both $\Delta R/R$ and $\Delta(R_\perp/R)$ show nonexponential decay and have tails longer than 10 ns. One can see that the first maximum of $\Delta R/R$ around 500 fs decrease with increase of T above 150 K. In contrast, $\Delta(R_\perp/R)$ has a conspicuous delayed peak at $t>1$ ns (indicated by closed triangles), which grows and shifts to longer delay times as T approaches the transition temperature T_{CO}.

The maximum values of $|\Delta R/R|$, plotted against T in Fig. 4(a), decrease steeply around 150 K, which is close to neither T_{CO} nor T_N (indicated by vertical broken lines). This behavior suggests that the CO/OO state becomes unstable upon photoexcitation below 150 K, which might be caused by a hidden ferromagnetic/metallic state competing with the antiferromagnetic CO/OO state.[17] Figure 4(b) shows the T dependence of the peak value and its delay time for the slow

component of $|\Delta(R_\perp/R)|$. The both quantities show critical enhancement as T approaches T_{CO}, reminiscent of the dynamical critical slowing down effect[18] as described below. In general, the initial state at temperature T_{ini} is determined by the minimum of the Ginzburg-Landau potential $G(\eta;T_{ini})$, where η is the order parameter. Let us consider that the temperature of the heat bath is slightly raised to T within a very short period, keeping the order parameter at the initial value, e.g., by ultrafast photoexcitation. Then the order parameter η relaxes to a new minimum of $G(\eta;T)$ in a manner such that $d\eta/dt=-L\partial G/\partial\eta$ (L being a positive constant) within the framework of the linear-fluctuation approximation. Since the minimum of G becomes shallower on approaching the transition temperature, the decay time constant is critically increased.

However, this naive picture with a single order parameter cannot be applied straightforwardly to the presently observed phenomena. This is because the photoexcitation at 1.55 eV corresponds to a charge transfer excitation from Mn^{3+} to Mn^{4+} so that the CO/OO state is immediately destroyed by photoexcitation. The difference in temporal behaviors as well as in temperature dependencies of $\Delta R/R$ and $\Delta(R_\perp/R)$ implies the existence of another order parameter. Although the charge/orbital order and the collective Jahn-Teller distortion are strongly tied to each other and hence can be regarded as a single order parameter in steady or slow phenomena, ultrashort photoexcitation can separate the dynamics of these two order parameters. The reflectivity change $\Delta R/R$ is mainly governed by the charge/orbital states, and hence represents almost genuine charge/orbital disorder. On the other hand, the optical anisotropy or birefringence signal $R_\perp/R$ has contributions from both the charge/orbital order and the collective Jahn-Teller distortion, the latter of which can give rise to the lattice orthorhombicity that is also responsible for optical anisotropy.

The dynamical critical slowing down observed in $\Delta(R_\perp/R)$ can be understood as that of the collective Jahn-Teller distortion order parameter η_{JT}. The adiabatic charge/orbital disorder can be induced without lattice relaxation immediately after photoexcitation, which should give rise to a similar temporal decay in $\Delta R/R$ and $\Delta(R_\perp/R)$ as observed at $t<10$ ps. Then, in accord with the adiabatic (constant-η_{JT}) excitation of the charge/orbital state, the electronic temperature is raised to T from T_{ini}, and the subsequent change in η_{JT} is described by the time-dependent Ginzburg-Landau equation mentioned above. During this process, the total energy of the system is relaxed to the equilibrium state with thermal diffusion, which is seen in the slow relaxation in the evolution of $\Delta(R_\perp/R)$. The delayed-peak intensity of $\Delta(R_\perp/R)$ can be related to the difference between the minimum positions of G at T_{ini} and T, and hence will be enhanced with increasing $d\eta_0/dT$ [$\eta=\eta_0$ giving the minimum of $G(\eta;T)$] or equivalently as T_{ini} approaches T_{CO}.

To summarize, the photoinduced effects on the CO/OO state have been investigated for a $La_{0.5}Sr_{1.5}MnO_3$ crystal by polarization-sensitive femtosecond pump-probe spectroscopy. The shift of the optical conductivity peak around 1.3 eV as well as the reduction of optical birefringence indicate the destruction of the CO/OO state by photoillumination. The temperature dependence of $\Delta R/R$ suggests that the CO/OO state becomes unstable below 150 K upon photoexcitation. The temporal evolution of birefringence $\Delta(R_\perp/R)$ in a two-step manner indicates the apparent separation of the order parameter in the charge/orbital sector and the lattice order parameter in the dynamic response. The charge/orbital order is first melted immediately upon the photoexcitation, giving rise to rapidly rising signals of both $\Delta R/R$ and $\Delta(R_\perp/R)$. Then the collapse of the collective Jahn-Teller distortion tends to follow the charge/orbital disorder and the resultant lattice disorder reaches a maximum in time in such a critically T-dependent manner as can be interpreted in terms of the critical slowing-down effect. Ultrafast spectroscopy is proved to be useful for investigating individual dynamics of order parameters that are strongly tied to each other in the static state.

This work was partially supported by a Grant-in-Aid for Centers of Excellence Research from the Ministry of Education, Science, Sports, and Culture of Japan, and by the NEDO of Japan.

*Present address: Department of Chemistry and Materials Science, Tokyo Institute of Technology, Tokyo 152-8551, Japan.

[1] J.M. Tranquada *et al.*, Phys. Rev. Lett. **73**, 1003 (1994); Phys. Rev. B **52**, 3581 (1995).

[2] C.H. Chen *et al.*, Phys. Rev. Lett. **71**, 2461 (1993); S.-H. Lee and S.-W. Cheong, *ibid.* **79**, 2514 (1997); H. Yoshizawa *et al.*, Phys. Rev. B **61**, R854 (2000).

[3] J.M. Tranquada *et al.*, Nature (London) **375**, 561 (1995); Phys. Rev. B **54**, 7489 (1996); J.M. Tranquada *et al.*, Phys. Rev. Lett. **78**, 338 (1997).

[4] See, for example, *Colossal Magnetoresistive Oxides*, edited by Y. Tokura (Gordon and Breach, Singapore, 2000).

[5] Y. Tokura and N. Nagaosa, Science **288**, 462 (2000).

[6] See, for example, *Ultrafast Spectroscopy of Semiconductors and Semiconductor Nanostructures*, 2nd ed., edited by Jagdeep Shah (Springer-Verlag, Berlin, 1999).

[7] See, for example, *Relaxation of Excited State and Photo-Induced Phase Transitions*, edited by K. Nasu (Springer-Verlag, Berlin, 1996).

[8] K. Miyano *et al.*, Phys. Rev. Lett. **78**, 4257 (1997).

[9] K. Matsuda *et al.*, Phys. Rev. B **58**, 4203 (1998).

[10] M. Fiebig *et al.*, Science **280**, 1925 (1998); Phys. Rev. B **60**, 7944 (1999); Appl. Phys. B: Lasers Opt. **71**, 211 (2000).

[11] Y. Moritomo *et al.*, Phys. Rev. B **51**, 3297 (1995).

[12] B.J. Sternlieb *et al.*, Phys. Rev. Lett. **76**, 2169 (1996).

[13] Y. Murakami *et al.*, Phys. Rev. Lett. **80**, 1932 (1998).

[14] K. Yamamoto *et al.*, Phys. Rev. B **61**, 14 706 (2000).

[15] T. Ishikawa *et al.*, Phys. Rev. B **59**, 8367 (1999).

[16] See, for example, M. Born and E. Wolf *Principles of Optics*, 7th ed. (Cambridge University Press, Cambridge, 1999).

[17] M. Tokunaga *et al.*, Phys. Rev. B **59**, 11 151 (1999).

[18] See, for example, E.M. Lifshitz and L.P. Pitaevskii, *Physical Kinetics* (Pergamon Press, Oxford, 1981).